INTERNATIONAL JOURNAL OF MARITIME TECHNOLOGY
IJMT Vol.15/ Winter 2021 (29-49)
Available online at: www. ijmt.ir

Evaluation of Optimal IM-EDP pairs for Typical South Pars Fixed Pile-Founded Offshore Platforms

Samira Babaei[1*], Rouhollah Amirabadi[2] , Mahdi Sharifi[3]

[1]*PhD Candidate, Department of Civil Engineering, University of Qom, Qom, Iran; S.Babaei@stu.qom.ac.ir*
[2]*Assistant Professor, Department of Civil Engineering, University of Qom, Qom, Iran; R.Amirabadi@ qom.ac.ir*
[3]*Assistant Professor, Department of Civil Engineering, University of Qom, Qom, Iran; M.Sharifi@ qom.ac.ir*

ARTICLE INFO

Article History:
Received: 11 Feb. 2021
Accepted: 19 Jun. 2021

Keywords:
Probabilistic Seismic Demand Model,
Probabilistic Seismic Demand Analysis,
Intensity Measures,
Engineering Demand Parameter, Fixed Pile-Founded Offshore Platform

ABSTRACT

Probabilistic seismic demand models (PSDMs) for typical South Pars fixed pile-founded offshore platforms, utilizing probabilistic seismic demand analysis (PSDA) have been presented in this study. It expresses the probability that a system experiences a certain level of engineering demand parameter (EDP) for a given intensity measure (IM) level. Utilizing Bin approach, 80 ground motion records have been selected. A three dimensional (3D) nonlinear model has been generated considering the effects of soil-pile-structure interaction (SPSI) and analyzed for each ground motion. The process involves a modal analysis to determine natural frequency as well as a static pushover analysis to establish yield values, and mode shape information, and finally 80 dynamic time-history analyses to determine demand, given IMs. With the probabilistic models being traditionally conditioned on a single seismic IM and single EDP, the degree of uncertainty in the models is dependent on the IM and EDP used. The present study evaluated optimal PSDMs build from 16 IMs against a wide range of EDPs in levels of local, intermediate and global. From a large combination of IM-EDP pairs, a selection of the optimal pairs has been made owing to the criteria of practicality, effectiveness, efficiency, and sufficiency. Results indicate the absolute superiority of velocity-related IMs compared to acceleration, displacement and time-related ones for most of EDP types. In particular, Housner Intensity-Global Drift and Specific Energy Density-Global Ductility (in global level), Housner Intensity-Jacket Drift (in intermediate level) and Housner Intensity- TopDeck Differential Settlement (in local level) result in optimal pairs. Conversely, $S_a(T_1, 5\%)$, the widely used IM in probabilistic assessment of fixed pile-founded offshore platforms, demonstrates relatively poor performance in predicting the demand parameters.

1. Introduction

Catastrophic failure caused by natural disaster such as hurricanes and earthquakes has led to severe damage to existing infrastructures, such as buildings, bridges and offshore platforms. Accordingly, it is of utmost importance to develop tools and techniques by which associated uncertainties involved in structural vulnerability assessment can be incorporated more efficiently. Since each type of infrastructure follows its own unique issues, a rational way to deal with this problem would be by investigating each category requisite, separately. Fixed pile-founded offshore platforms are now being installed in seismically active and environmentally sensitive regions1. Failure probability of offshore platforms under various levels of seismic excitation may affect not only the oil and gas production activity or the safety and serviceability of the platform but it may also have detrimental environmental effects. Furthermore, it is desirable that the risk of seismic damage be on par with risks due to other hazards such as explosion, fire and so on.[1] Few studies have considered the impact of uncertainty inherent to offshore structures, which have the common complexity of geometric uncertainties found in common building structures in addition to the complexity of parameters uncertainties inherent in soil–pile structure interaction (SPSI). Overall structural response and capacity of fixed pile-founded offshore platform greatly depends on the member behavior in the nonlinear range of deformation and the non-linear interaction of the driven piles with the surrounded soil.[2] Nonlinear behavior and the ultimate strength of fixed pile-founded offshore platforms under earthquake excitation have been the subject of a number of

researches.[3-5] Analytical model of an offshore structure was employed in the study of Asgarian et al.[6] to assess the performance of an offshore structures using Incremental Dynamic Analysis (IDA).[7] Proposed by Ajamy et al.[8] a comprehensive extended IDA method was carried out to incorporate different sources of uncertainty in the stochastic seismic analysis of fixed offshore platforms. The effect of uncertainties associated with the design of a fixed pile-founded offshore platform was investigated through FOSM and Tornado diagram methods in the study of El-Din and Kim.[2] Elsayed et al.[9] presented an approach for the reliability assessment of a fixed pile-founded offshore platform against earthquake collapse considering SPSI. Anderson-Darling (AD) goodness of fit test[10], was employed so as to investigate the assumption of lognormal hypothesis for the drift demand of fixed pile-founded offshore platforms at two different regions of IM by Abyani et al.[11] Quantitatively investigating the effects of sample size of records on seismic performance of fixed pile-founded offshore platforms, Abyani et al.[12], employed generic algorithm. Their drawn results proved that the fragility curves based on the suites with larger sample sizes are closer to the target fragility. It is worth considering that aforementioned studies, used $S_a(T_1, 5\%)$ as the intensity measure (IM) in incremental dynamic analysis (IDA) of fixed pile-founded offshore platforms.

Performance- Based Earthquake Engineering (PBEE) framework was first introduced by Cornell and Krawinkler[13], which have been used in many studies in order to evaluate the seismic structural performance, taking into account both aleatory and the epistemic uncertainties. One of its basic components is the probabilistic seismic demand model (PSDM). PSDM is based upon a representative relation between ground motion intensity measures (IMs) and engineering demand parameters (EDPs) according to Probabilistic Seismic Demand Analysis (PSDA). Probabilistic seismic demand analysis (PSDA) of nonlinear structures was performed by Shome[14] and Shome and Cornell.[15] Although a great deal of research has been made in the case of bridge and building structures, relatively limited effort has been focused to develop PSDMs for onshore and offshore structures based on PSDA. Luco[16] used a combination of two IMs to account for the effects of near-field ground motions on nonlinear structural responses. Gardoni et al.[17], proposed a general Bayesian methodology to construct probabilistic models that account for any source of information, including field measurements, laboratory data and engineering judgement. Mackie and Stojadinović[18] conducted a sensitivity analysis to explore the effect of different ground motion intensities on the seismic demands of reinforced concrete (RC) bridges. Gardoni et al.[19], Zhong et al.[20] and Huang et al.[21], constructed PSDMs for RC bridges. Padgett et al.[22] evaluate optimal IMs for use when generating probabilistic seismic demand models for bridge portfolios. Development of the port system risk analysis framework, have been described by Werner et al.[23] and Rix et al.[24]. Besides, seismic vulnerability and fragility curves for pile-supported wharves is developed in some researches.[25-27] Amirabadi et al.[28] developed optimal PSDMs for pile-supported wharf structures with batter piles, employing PSDA. A comprehensive Bayesian framework and fragility estimations for un-anchored steel storage tanks in petroleum complexes has been performed by Berahman and Behnamfar.[29] The use of a multivariate demand model for non-structural components was proposed by Lucchini et al.[30]. Moreover, to extend the definition of PSDM to concrete dams, a research was carried out by Hariri-Ardebili and Saouma.[31] Kaynia[32] demonstrated the performance-based seismic consideration of offshore wind turbines. Furthermore, Kia et. al[33] employed PSDA and developed a reliability-based seismic demand curve of a sample 4-story building.

It can be interpreted that among broad usage of PSDA for evaluating buildings and bridges, almost none of the related researches has hinted to this approach for fixed pile-founded offshore platforms, nevertheless.

This method attempts to signify seismicity through a wide selection of many ground motions and their IMs, grouped into bins against corresponding value of the extensive variety of EDPs. Probabilistic seismic demand models (PSDMs) generated by employing PSDAs provided by several IM-EDP pairs among which the optimal combination is selected.[18] The focus of attention for developing optimal IM-EDP pairs according to optimal models for the class of fixed pile-founded offshore platforms installed/designed to be installed in the South Pars Oil and Gas Field located in the Persian Gulf, analyzed in the present study, made the optimal PSDM implemented by PSDA, to become a very powerful tool in performance-based seismic design and evaluation of this type of structures. This study aims to represent a comprehensive probabilistic seismic assessment of fixed pile-founded offshore platforms located in the Persian Gulf designed according to the provisions of the API, American Petroleum Institute Recommended Practice for Planning[34].The proposed method overview is implemented in Figure 1.

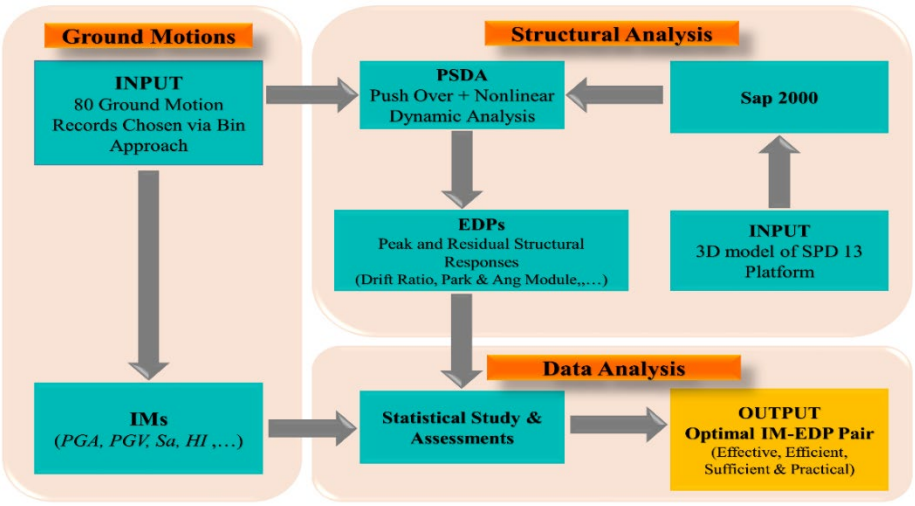

Figure 1. Overview of the Optimal PSDM Evaluation Proposed for the typical South Pars Offshore Platforms

2. Probabilistic Seismic Demand Model

Performance-Based Earthquake Engineering (PBEE) describes the quantitative means for achieving predetermined performance levels in specific earthquake intensities. Pacific Earthquake Engineering Research (PEER) centre has developed a probabilistic framework for performance-based design and evaluation.[14] One of the basic components of the PBEE framework is the probabilistic seismic demand model (PSDM). PSDM is based upon a representative relation between IMs and EDPs.

Total probability theorem is used by the PEER–PBEE framework through which the problem is de-aggregated into several interim probabilistic models. Therefore, the sources of randomness and uncertainty are addressed more rigorously. In this study, one component of the de-aggregated PEER–PBEE equation, the interim demand model or the relation between structural demand and earthquake intensity is discussed. A PSDM, is used to estimate the mean annual frequency (ν) of exceeding a given structural engineering demand parameter (EDP > edp) in a postulated hazard environment (IM > im), expressed as follows:

$$\nu(EDP \geq edp) = \int_{edp} G(EDP \geq edp|IM = im)|d\lambda(im)|, \quad (1)$$

Where, $G(EDP \geq edp|IM = im$ is the demand model which predict the exceeding probability of an engineering demand parameter (edp) for a seismic hazard intensity measure (im). $\lambda(im)$ is the seismic hazard model to predict the annual exceeding probability of seismic hazard intensity measure (im) in a seismic hazard environment.

A PSDM is a result of probabilistic seismic demand analysis (PSDA). PSDA, as defined by Shome et al.[35], is the coupling of probabilistic seismic hazard analysis (PSHA) and nonlinear structural analysis. PSDA used to formulate a PSDM that applies to an entire region, rather than to a unique location; applies to an array of possible decision variables, rather than a single one; and applies to a class of structures, rather than to a unique structure. Such PSDMs are quite general. The procedure used to formulate them has four aspects: choice of ground motions, definition of the class of structures, formulation of a nonlinear analysis model, and choice of IM and EDP pairs to describe the model.

3. Ground Motion Records and Intensity Measures for PSDA

3.1 Record Selection

Not being based on seismic hazard curves, PSDA uses a ground motion bin approach instead.[15,35] It would also be possible to perform the analysis using a standard Monte Carlo simulation[36] involving thousands of ground motions, or by generation of synthetic ground motions. The bin approach chooses a suite of ground motions typical for the region under study from a database of recorded ground motions.

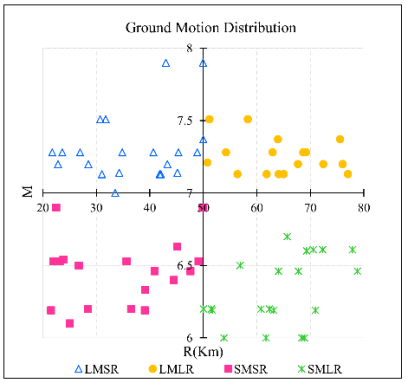

Figure 2. Distribution of Ground Motion Records in M_w-R Space

Separating bins by magnitude and epi-central distance makes this strategy comparable to conventional PSHA.

One advantage of using bins is the ability to abstract individual earthquakes and consider the effect of generalized earthquake characteristics, such as frequency domain content, dominant period, or duration, on structural demand. Ground motion intensity can also be abstracted by scaling the earthquakes in a bin to the same level of intensity. More importantly, the bin approach provides a way to limit the number of ground motions in the suite. Shome et al.[35] showed that, assuming a log-normal probability distribution of structural demand measures, the number of ground motions sufficient to yield response quantity statistics that have a required level of confidence is proportional to the square of a measure of dispersion of demand measure data. They also showed that proper scaling of bin intensities can reduce dispersion, and thus substantially reduce the number of ground motions required for confident analysis. Finally, they showed that the bin approach by itself does not introduce bias into the relation between structural demand measures and ground motion intensity measures.

In this study, four bins with 20 non-near-field ground motions each were obtained from the PEER Strong Motion Database has been selected.[37]

The delineation between small (SM) and large (LM) magnitude bins was at Mw = 7. Ground motions with closest distance R ranging between 20 and 50 km were grouped into a small distance (SR) bin, while ground motions with R > 50 km up to 80 km were in the large distance (LR) bin. All ground motions were recorded on NEHRP soil type C sites.[38] The distribution of motions is shown in Figure 2. The details of all ground motion records, the name of earthquakes, sensor location, magnitude and distance are presented in Table 1.

Table 1. Characteristic of Selected Ground Motion according to Bin Approach

	Event	Year	M	R(km)	Station
LMLR	Trinidad	1980	7.2	76.06	Rio Dell Overpass-FF
	Trinidad	1980	7.2	76.06	Rio Dell Overpass-E Ground
	Trinidad	1980	7.2	76.06	Rio Dell Overpass-W Ground
	Landers	1992	7.28	69.21	Amboy
	Landers	1992	7.28	62.98	Fort Irwin
	Landers	1992	7.28	68.66	Hemet Fire Station
	Landers	1992	7.28	54.25	Indio-Coachella Canal
	Kocaeli, Turkey	1999	7.51	58.33	Hava Alani
	Kocaeli, Turkey	1999	7.51	51.17	Mecidiyekoy
	Caldiran,Turkey	1976	7.21	50.78	Maku
	Manjil, Iran	1990	7.37	75.58	Abhar
	Manjil, Iran	1990	7.37	63.96	Rudsar
	Hector Mine	1999	7.13	64.08	Baker Fire Station
	Hector Mine	1999	7.13	61.85	Big Bear Lake- Fire Station
	Hector Mine	1999	7.13	77.01	Cabazon
	Hector Mine	1999	7.13	56.4	Desert Hot Spring
	Hector Mine	1999	7.13	65.04	Fort Irwin
	Hector Mine	1999	7.13	61.86	North Palm Spring Fire Sta.
	El Mayor- Cucapah	2010	7.2	72.44	Salton City
	El Mayor- Cucapah	2010	7.2	67.71	Ocotillo Wells – Veh. Rec. Area
LMSR	Landers	1992	7.28	34.86	Barstow
	Landers	1992	7.28	21.78	Desert Hot Spring
	Landers	1992	7.28	26.96	Mission Creek Fault
	Landers	1992	7.28	23.62	Yermo Fire Station
	Gulf of Aqaba	1995	7.20	43.29	Eilat
	Kocaeli, Turkey	1999	7.51	31.74	Goynuk
	Kocaeli, Turkey	1999	7.51	30.73	Iznik
	Duzce,Turkey	1999	7.14	34.30	Mudurnu
	Duzce,Turkey	1999	7.14	45.16	Sakarya
	Manjil, Iran	1990	7.37	49.97	Qazvin
	Hector Mine	1999	7.13	41.81	Amboy
	Hector Mine	1999	7.13	31.06	Joshua Tree
	Hector Mine	1999	7.13	42.06	Twenty nine Palms
	Denali, Alaska	2002	7.90	49.94	Carlo (temp)
	Denali, Alaska	2002	7.90	42.99	R109 (temp)
	Landers	1992	7.28	45.34	Forest Fall Post Office
	Landers	1992	7.28	48.84	Indio - Jackson Road
	Landers	1992	7.28	40.67	Morongo Valley Hall
	El Mayor- Cucapah	2010	7.20	28.53	El Centro – Meloland
	El Mayor- Cucapah	2010	7.20	22.83	El Centro Differential Array

SMLR	Borrego	1942	6.5	56.88	El Centro Array #9
	Ierissos, Greece	1983	6.7	65.67	Ierissos
	Morgan Hills	1984	6.19	51.68	APPLE 1E-Hayward
	Morgan Hills	1984	6.19	63.16	Los Banos
	Morgan Hills	1984	6.19	70.93	SF Intern. Airport
	Big Bear - 01	1992	6.46	78.81	Featherly Park – Maint
	Big Bear - 01	1992	6.46	67.74	Mt Baldy – Elementary Sch.
	Big Bear - 01	1992	6.46	64.04	Phelan – Wilson Ranch
	Chi-Chi, Taiwan-04	1999	6.2	50.02	CHY015
	Chi-Chi, Taiwan-04	1999	6.2	60.77	TCU117
	Chi-Chi, Taiwan-04	1999	6.2	51.48	TCU118
	Chi-Chi, Taiwan-04	1999	6.2	62.35	TTN044
	Tottori, Japan	2000	6.61	70.55	HRS010
	Tottori, Japan	2000	6.61	72.30	HRS015
	Tottori, Japan	2000	6.61	77.85	SMN017
	Bam, Iran	2003	6.6	69.28	Jiroft
	Parkfield-02, CA	2004	6.0	61.72	San Luis Obispo
	Parkfield-02, CA	2004	6.0	68.85	Cambria – Hwy1Caltrans Bridge
	Parkfield-02, CA	2004	6.0	53.87	KING CITY– CANAL
	Parkfield-02, CA	2004	6.0	68.38	Greenfield – Police Station
SMSR	Northern Calif - 01	1941	6.4	44.52	Ferndale City Hall
	Northern Calif - 01	1954	6.5	26.72	Ferndale City Hall
	Borrego Mtn	1968	6.63	45.12	El Centro Array #9
	Imperial Valley - 06	1979	6.53	23.17	Calipatria Fire Station
	Imperial Valley - 06	1979	6.53	49.1	Coachella Canal #4
	Imperial Valley - 06	1979	6.53	22.03	Delta
	Imperial Valley - 06	1979	6.53	21.98	El Centro Array #13
	Imperial Valley - 06	1979	6.53	35.64	Niland Fire Station
	Victoria, Mexico	1980	6.33	39.1	SAHOP Casa Flores
	Morgan Hills	1984	6.19	39.08	Capitola
	Chalfant Valley – 02	1986	6.19	21.55	Benton
	Superstition Hills	1987	6.54	23.85	Wildlife Liquifaction Arrey
	Big Bear - 01	1992	6.46	47.6	Hemet Fire Station
	Big Bear - 01	1992	6.46	40.87	North Palm Springs #36
	Kobe, Japan	1995	6.9	49.91	Chihaya
	Kobe, Japan	1995	6.9	22.5	Kakogawa
	Chi-Chi, Taiwan 04	1999	6.2	28.45	CHY034
	Chi-Chi, Taiwan 04	1999	6.2	36.48	TCU141
	Joshua Tree, CA	1992	6.1	25.04	Indio – Jackson Road
	Darfield, New Zealand	2010	7	33.54	MAYC

3.2 IM Selection

Sixteen IM candidates from literature are examined for probabilistic seismic demand analysis of the fixed pile-founded offshore platforms. Table 2 summarizes and categorizes them into two main groups: (1) non-structure specific (derived from time history) and (2) structure specific (derived from spectrum, for example). Based on the definitions of these IMs, they are further classified into various categories such as acceleration-related, velocity-related, displacement-related and time-related. Besides, it is well known that a ground motion is characterized by its amplitude, frequency content, and duration.[39] Among the studied IMs in Table 2, some describe only one of these characteristics, while others reflect two or three. For example, peak quantities (e.g., *PGA*, *PGV* and *PGD*) account for the ground motion amplitude only; cumulative quantities such as *CAV* account for both amplitude and duration features, while Arias intensity (I_a) and root-mean-square (*RMS*) of acceleration, velocity and displacement account for all the three features. On the other hand, spectral terms account for both amplitude and frequency content characteristics.

Table 2. Intensity Measures considered in this study

IM	Name	Definition
	Non-Structure Specific	
Acceleration-Related		
PGA	Peak Ground Acceleration (g)	$Max\|a(t)\|$, *a(t)* is acc. time history
CAV	Cumulative Absolute Velocity[56]	$\int_0^{t_{tot}}\|a(t)\|\,dt$, t_{tot} is the total duration
I_a	Arias Intensity[57]	$(\pi/2g).\int_0^{t_{tot}} a^2\,(t)dt$
A_{rms}	*Root-mean square (RMS) of Acceleration*	$\sqrt{\frac{1}{t_d}\int_{t_1}^{t_2} a^2\,(t)dt}$, t_1 , t_2 & t_d seen in *SD*
Velocity-Related		
PGV	Peak Ground Velocity (m/sec)	$Max\|v(t)\|$, *v(t)* is velocity time history
V_{rms}	RMS of Velocity	$\sqrt{\frac{1}{t_d}\int_{t_1}^{t_2} v^2\,(t)dt}$
SED	Specific Energy Density	$\int_0^{t_{tot}} v^2\,(t)dt$
Displacement-Related		
PGD	Peak Ground Displacement	$Max\|u(t)\|$, *u(t)* is displacement time history
D_{rms}	RMS of displacement	$\sqrt{\frac{1}{t_d}\int_{t_1}^{t_2} u^2\,(t)dt}$
Time-Related		
$\frac{V_{max}}{A_{max}}$	Peak velocity/Acceleration ratio	$\frac{PGV}{PGA}$
	Structure Specific	
Acceleration-Related		
S_a	Spectrum Acceleration (g)	
PS_a	Pseudo Acceleration	
Velocity-Related		
S_v	Spectrum Velocity (m/sec)	
PS_v	Pseudo Spectrum Velocity	
HI	Housner Intensity[58]	$\int_{0.1}^{2.5} PS_v\,(\xi = 5\%, T)dT$
Displacement-Related		
$\boldsymbol{S_d}$	**Spectrum Displacement**	

4. PSDA CLASS OF STRUCTURES AND STRUCTURAL EDPS

4.1 Class of Structures

The second step of the PSDMs formulation is the classification of structures and determination of structural EDPs. In this study, a class of four leg fixed pile-founded offshore platforms installed/designed to be installed in the South Pars Oil and Gas Field of the Persian Gulf has been selected so as to obtain the optimal IM-EDP pairs. Aforementioned platforms generally consist of the following main parts: 1. Superstructure providing deck space for supporting operational appurtenances and other loads. 2. Completely braced, redundant welded tubular space frame extending from an elevation at or near the sea bed to above the water surface, which is designed to serve as the main structural element of the platform, transmitting lateral and vertical forces to the foundation (jacket). 3. Piles that permanently anchor the platform to the ocean floor, and carry both lateral and vertical loads.

4.2 Engineering Demand Parameter

The type and function of the offshore platform in addition to the platform modes of failure, are the main factors in selecting the appropriate engineering demand parameter (EDP). EDP characterizes the response of the structure under investigation subjected to a

prescribed seismic loading. In other words, EDP represents the output of the corresponding nonlinear dynamic analysis. It should be specified properly considering the characteristics of the structural system under investigation and satisfactory related to structural damage.

As mentioned, fixed pile-founded offshore platform is a multi-part multi-environment structure consisting of three main parts. The structural integrity will be maintained based on the accurate behavior of the connections under sever loading conditions. Consequently, monitoring the nonlinear response of below deck columns (which are connecting the deck to the jacket) and mudmat (as the separator of jacket and pile foundation) seems to be vital. On the other hand, nonlinearity in piles and buckling of the struts are important issues which have to be considered. Moreover, it should be noticed that the deck in an offshore platform is of the utmost importance due to expensive deck equipment and modules required for operation as in the case of riser platforms or well head platforms. Besides, the deck appurtenances are heavy and most of them are acceleration sensitive. Accordingly, any unpreserved deck displacement which is not kept within a certain limit states, will probably lead to the detrimental domino effects caused by dropping objects, fire, blast and so on.

Based on the platform type, fundamental period and modes of failure, for each main part of the platform, different EDPs is considered. On the other hand, EDPs are described as local (e.g. peak or residual member displacement), intermediate (e.g. pile drift ratio) and global (e.g. global ductility) response quantities. In a fixed pile-founded offshore platform, local EDPs refer to the individual member response of each main part (deck, jacket and pile), since the intermediate EDPs express the overall response of each main part not including the effect of other main parts responses. Finally, Global EDPs, states those responses in which the whole structure and the effect of each main part to others are involved. Fixed pile-founded offshore platform EDPs and their range as local, intermediate and global are tabulated in Table 3.

Table 3. Engineering Demand Parameters

Range	Name	Formula	Units
	Yield Displacement	u_y	m
	Yield Curvature	ϕ_y	1/m
	Yield Energy	$E_y = \int_0^{u(\max(F))} F(u)du$	
Local (Frame)	Maximum Horizontal Disp.	$u_{(x,y)max} = max\left(\lvert u_{(x,y)}(t)\rvert\right)$	m
Local	Max Settlement	$u_{(z)max} = max(\lvert u_z(t)\rvert)$	m
Intermediate(stories), **Global**(deck, jacket, pile, platform)	Max Horizontal Differential Disp.	$du_{(x,y)max} = max\left(\lvert u_{(x,y)j}(t) - u_{(x,y)i}(t)\rvert\right)$	m
Intermediate, Global	Max Differential Settlement	$du_{(z)max} = max(\lvert du_z(t)\rvert)$	m
Local, Intermediate, Global	Drift Ratio	$\theta = \frac{u_{(x,y)max}}{H}$	%
Local	Max Curvature	$\phi_{max} = max(\lvert\phi\ (t)\rvert)$	1/m
Local	Max Moment	$M_{max} = max(\lvert M\ (t)\rvert)$	KN.m
Local, Intermediate, Global	Residual Horizontal Disp.	$u_{(x,y)res} = max(\lvert u_{(x,y)}(t_{max})\rvert)$	m
Local	Res. Settlement	$u_{(z)res} = max(\lvert u_{(z)}(t_{max})\rvert)$	m
Intermediate, Global	Res. Horizontal Differential Disp.	$du_{(x,y)res} = max(\lvert du_{(x,y)}(t_{max})\rvert)$	
Intermediate, Global	Res. Differential Settlement	$du_{(z)res} = max(\lvert du_{(z)}(t_{max})\rvert)$	
Intermediate, Global	Res. Disp. Index	$RDI = \frac{u_{res}}{u_y}$	%
Intermediate, Global	Disp. Ductility	$\mu_\Delta = \frac{u_{(x,y)max}}{u_y}$	-
Intermediate, Global	Plastic Rotation	$\theta_{pl} = \frac{u_{(x,y)max} - u_y}{H}$	rad
Global	Hystertic Energy	$HE = \oint_\theta M(\theta)d\theta$	

Local, Intermediate	Soil Link Deflection	m
Local, Intermediate	Soil Link Force	KN
Local (equipment), **Intermediate** (Deck Stories), **Global** (Top of the Structure	Acceleration	g
Intermediate, Global	Base Function	KN
Local, Intermediate	Frame Force	KN
Local	Plastic Hinges Formation	

It is worth noticing that, most of the conducted researches have not considered the deck part and its equipment besides their aforementioned importance. According to literature, apart from the peak displacement at top of the jacket, the global drift ratio is commonly accepted criterion for the global level performance of the structures. In offshore platform structures limiting global drift ratio to appropriate values would prevent brace buckling besides maintaining the functionality of risers and conductor systems. It is also worth considering that in case of buildings, maximum inter-level drift ratio may be selected knowing the fact that foundation rotations are not severe. Moreover, utilizing maximum inter-level drift ratio, lead to avoid non-structural damage to the building by setting appropriate limit states and preventing the exceedance of drift from certain values. While for offshore platforms, some other aspects should be taken into account and EDPs should be selected depending primarily upon the type of the platform. Additionally, candidate EDPs should account for both brace buckling as well as pile failure. The former can be taken into account by peak inter-story drift whilst the latter requires more investigations.[6] Among proposed EDPs in Table 3, these EDPs have been used in recent researches: (a) Inter-level drift ratio, by which buckling of braces in any type of structure can be captured, (b) Peak drift from mud line up to deck level which is a suitable parameter to account for both brace buckling besides pile failure in most geotechnical conditions, (c) Peak displacement at top of the jacket and (d) Overall drift from the lower level of the pile under the ground up to the deck level.[2,6] Asgarian et al.[6] showed that the latter does not appear to be so representative since different forms of deformation of pile may take place when subjected to external actions.

5. DESCRIPTION OF THE MODEL STRUCTURE

5.1 Analysis Model Description

The key characteristics of the base model are presented in the Table 4. The studied model is a X brace four leg battered fixed pile-founded platform with four main piles recently installed in the 13th Phase, South Pars Oil and Gas Field of the Persian Gulf in (-57.2) meter water depth and the pile foundations penetrate 106 meters below mudmat. To obtain accurate results, three dimensional model of the platform has been taken into consideration and the model is subjected to ground motion excitations in both X and Y directions.

Table 4. General arrangement of the model

Jacket Geometry	4 leg jacket with 4 main piles
Leg Batter	Row 2: single 1:7, Row 1: double 1:7 & 1:8
Leg Spacing	20 m × 13.716 m at work point
Foundation	Four driven piles grouted to jacket legs
Jacket Framing Elevations	
Work Point	EL. (+) 8.300 m
Level-1 (Sea Deck)	EL. (+) 5.750 m
Level-2	EL. (-) 15.000 m
Level-3	EL. (-) 36.000 m
Level-4	EL. (-) 57.200 m
Wellhead Framing Level	EL. (+) 10.050 m
Deck Elevations	
Top Deck with Helideck	EL. (+) 26.725 m
Upper Deck	EL. (+) 22.645m
Lower Deck	EL. (+) 18.900 m
Cellar Deck	EL. (+) 13.900 m

5.2 The Pile Surrounded Soil Layer Characterization

According to the field and laboratory investigations, the stratum encountered at the borehole performed at the platform location was very soft calcareous becoming carbonate clay (CH) overlying medium dense becoming loose clayey siliceous carbonate sand (SC) at 10.60m. More detailed of the pile surrounded soil profile is presented in the Table 5.

Table 5. Soil Layer Characteristics

Unit	Depth below Seafloor (m)		Generic Soil Description	γ' (Kn/m^3)
	From	To		
1a	0.00	3.50	Very Soft CLAY	5.8
1b	3.50	10.60	Very Soft CLAY	7.3
2a	10.60	12.60	Medium dense clayey siliceous carbonate SAND	9.4
2b	12.60	14.10	Loose clayey siliceous carbonate SAND	9.4
3	14.10	15.20	Firm CLAY	8.5
4	15.20	17.20	Medium dense silty siliceous SAND	8.9
5a	17.20	20.00	Firm to soft CLAY	7.5
5b	20.00	24.80	Soft to firm CLAY	8.8
6a	24.80	27.80	Stiff CLAY	9.5
6b	27.80	40.00	Stiff CLAY	8.8
6c	40.00	42.20	Stiff CLAY	9.6
7a	42.20	43.66	Very dense clayey siliceous carbonate SAND	10.0
7b	43.66	45.10	Dense clayey siliceous carbonated SAND	10.0
8	45.10	47.00	Hard sandy CLAY	9.5
9a	47.00	52.00	Very stiff CLAY	10.0
9b	52.00	53.50	Very stiff CLAY	10.2
10	53.50	54.00	Dense cemented siliceous carbonate SAND	10.2
11a	54.00	56.50	Very stiff CLAY	9.9
11b	56.50	57.50	Stiff CLAY	9.9
12a	57.50	59.70	Dense locally moderately cemented clayey siliceous carbonate GRAVEL	9.5
12b	59.70	61.60	Medium Dense Clayey siliceous carbonate GRAVEL	9.6
13a	61.60	79.50	Very stiff CLAY	9.5
13b	79.50	89.80	Very stiff CLAY	10.0
14	89.80	90.65	Very dense locally cemented clayey siliceous carbonate SAND	9.6
15a	90.65	98.00	Hard CLAY	9.5
15b	98.00	105.3	Hard CLAY	9.3
16	105.3	110.40	Hard CLAY	10.3

5.3 Modeling of piles

Structural behavior of offshore platform in the nonlinear range depends primarily on the soil–pile–structure interaction (SPSI). Several simplified methods have attempted to capture the main aspects of SPSI, considering the fact that the seismic performance of soil and pile foundations is a complex issue. Utilized in the present study, the Beam on Nonlinear Winkler Foundation (BNWF) model, has been of a major concern.[40] Often referred to as the p-y method, this model use parallel nonlinear soil–pile springs along the pile penetration length to approximate the interaction between the pile and the surrounding soil.[41,42] It is worth considering that the BNWF model simplifies the interaction between the soil and the pile assuming that the displacement of one spring has no effect on other springs displacement. The lateral soil stiffness is modelled using the p–y approach. In this approach, for each layer of soil along the depth, a nonlinear relationship is established between the pile lateral displacement (y) which mobilizes the lateral soil reaction (p) per unit length. In cohesive soils p-y curve data has been generated using the methods prescribed in API[34] and Matlock[40]. On the other hand, the p-y data for the granular soils of greater than 50% measured carbonate content, is based on the recommendations in Wesselink et al.[43] In the present study, p–y curves are based on the actual soil data extracted from the geotechnical report of the platform site. Sap 2000[44] multi-linear plastic type link element is employed in the numerical model proposed in this paper so as to model the nonlinear lateral relation between the soil and the pile. In that link element, the nonlinear link stiffness for the axial degree of freedom is defined according to the p–y curve. Then the p–y curve is redefined as a force–deformation relationship in which p is the total force acting along the tributary length of a pile joint. In order to represent the lateral soil nonlinear behavior, a lateral link is defined for each joint along each unit pile segment. Chosen from the SAP2000 library, a multi-linear kinematic plasticity property type used for uniaxial deformation. The selected property models the hysteresis of the non-gapping soil behavior. Besides lateral loads, the pile foundation is exposed to the static and cyclic axial loads. Nonlinear axial load-deformation behavior along the shaft of driven tubular pile may be modelled using t-z data, recommended by API RP 2A-WSD.[45] Similarly, q-z curves model the elastic and plastic soil deformations around the pile tip so as to reflect the relationship between mobilized end bearing resistance and axial tip deflection. The nonlinear load-displacement relationships and spring parameters (q-z data) for the studied platform location are generated based on the recommendations contained in API RP 2A-WSD[45] according to the site investigation and pile testing data. The skin friction and the end bearing between a pile and the surrounding soil produce the soil resistance to the axial movement of the pile.[46-48] The schematic configuration of the proposed model in SAP2000 is illustrated in Figure 3.

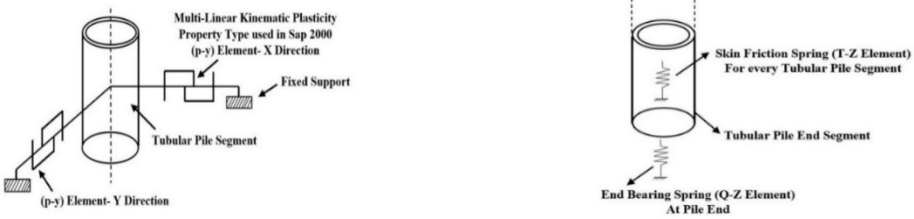

(a). P-Y Elements **(b).** T-Z and Q-Z Elements

Figure 3. Schematic configuration of pile segments and (a) P-Y elements, (b) T-Z & Q-Z elements

To model the behavior of a pile, frame elements are chosen from the library of the SAP2000. The outer diameter of the pile is uniformly 1524 mm while the thickness of the wall varies. In order to simulate the structure–pile–soil interaction through several layers of different soils, the piles are divided along their vertical axis.

5.4 Seismic site response analysis

Even at relatively small strains, soil exhibit small nonlinear behavior. Thus, it is necessary to incorporate soil nonlinearity in any site response analysis. Each soil layer is characterized by its thickness, mass density, shear wave velocity, and nonlinear soil properties including nonlinear modulus reduction and damping curves which effect on the selected ground motion records. Seismic site response analysis evaluates the influence of local soil conditions through shear wave propagation within horizontal soil layers. In fact, the results of site response display seismic performance assessment of nonlinear ground response analysis within the soil profile, while they can reflect uncertainties in determination of the input ground motions, characterization of the site velocity profile and specification of the nonlinear properties as well as selection of the technique of analysis.[49] The computer program DEEPSOIL is employed so as to perform site response simulations based on the soil layer characteristics and selected ground motion records.[50] DEEPSOIL uses one dimensional nonlinear time domain analysis which is computationally efficient and requires meaningful input data such as shear-wave velocity and the nonlinear soil properties. This program performs nonlinear site response analysis using outcropping motions in the time domain and the layered soil column as a multiple-degree-of-freedom lumped mass system. The definition of soil sub-layers is based upon their thickness, unit weight, shear wave velocity and material properties. The soil response is obtained from a constitutive model that describes the cyclic behavior of soil. It is worth noting that, different solutions have been and continue to be developed to solve the propagation of shear waves throughout a non-linear soil profile; these solutions have been used to develop a variety of site response analysis software.

The schematic illustration of the platforms is shown in Figure 4(a) in which soil layers, p-y, t-z and q-z springs, multi-degree-of-freedom lumped parameter model and displacement time history from nonlinear site response analysis are considered. Figure 4 (b), (c) and (d), shows deck, jacket and pile sections, respectively, in which the schematic deformed shape views are included. The platform appurtenances comprise the non-structural members such as flooding system, centralizer, pad-eyes, plates and stiffeners, etc. The analysis models include only the major structural components, and the contribution of the conductors to the platforms' stiffness and strength is neglected. The frame elements, considered as jacket horizontal members are rigidly connected at the ends. The dynamic model of fixed pile-founded offshore platforms should reflect the key analytical parameters of mass, damping, and stiffness.

The accurate mass consideration should include that of the platform steel, all deck loads, conductors, and appurtenances, the mass of water enclosed in submerged tubular members (added mass) and the mass of marine growth expected to accumulate on the structure (increased member diameter due to marine growth).[34] The three dimensional (3D) models have been created employing Sap 2000, drag and inertia forces were exerted and modal, static push over (SPO) and nonlinear time history (NTH) analysis have been carried out. Numerous quantities were monitored in order to extract maximum and residual dynamic quantities, such as axial force, moment, horizontal and vertical displacements and so on. Any number of response quantities can be extracted from the model by post-processing.

Table 6. Comparison of the First Three Periods in Sap 2000 and SACS

	Period	Sap 2000(s)	SACS(s)
SPD 13, 3D Model, Modal Analysis	1st Mode	2.26	2.38
	2nd Mode	1.96	2.03
	3rd Mode	1.51	1.43

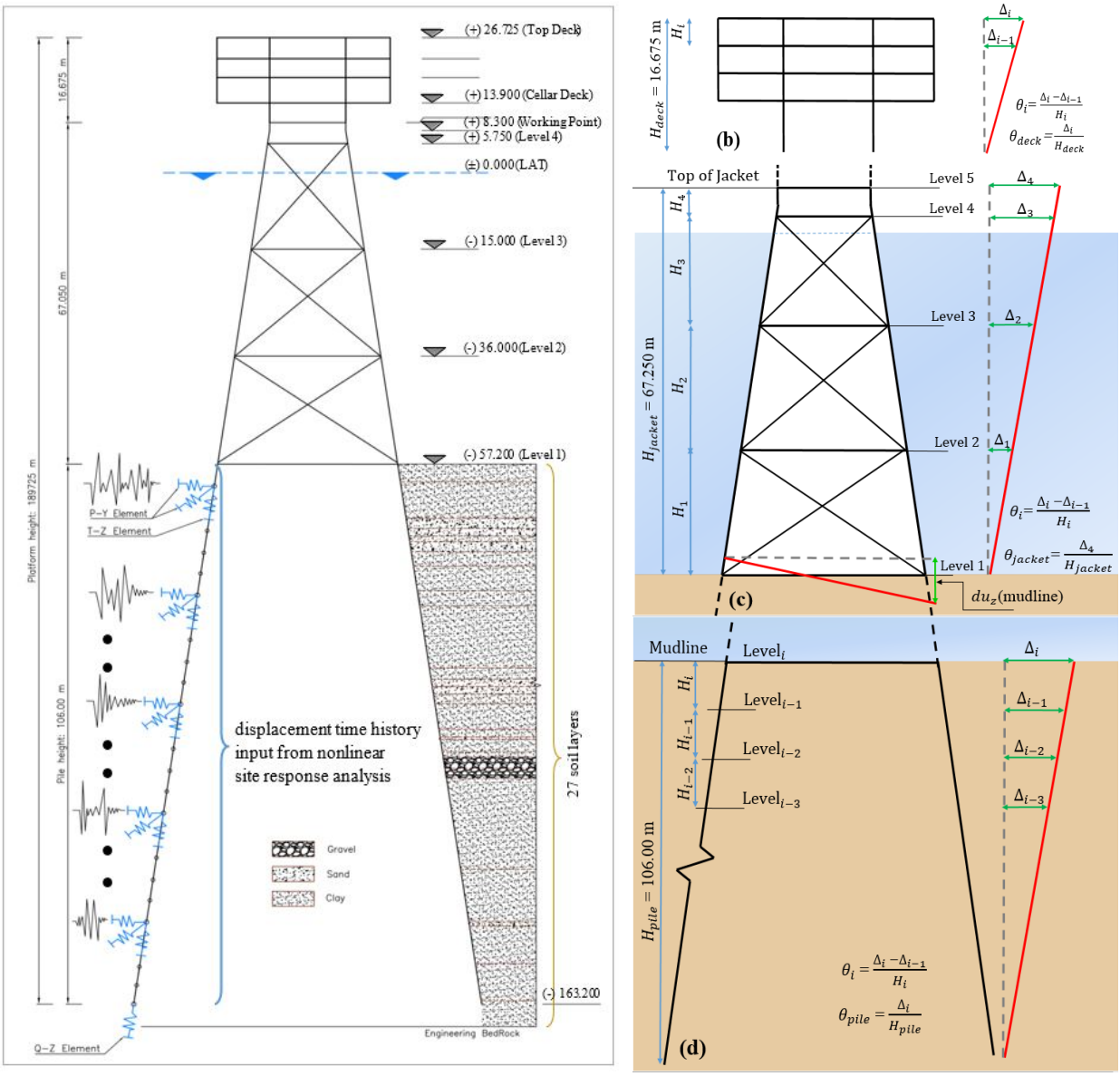

Figure 4. A schematic 2D view of platform (a). Soil layers, SPSI and multi-degree-of-freedom lumped parameter model shaken at the base, (b). Deck section, (c). Jacket section, (d). Pile section

Figure 5 illustrates the first three modes in the 3D model of studied fixed pile-founded offshore platform in both (a) xy view and (b) yz view and the periods of the first three vibration modes for the studied platform is listed in Table 6. Evident from the table, Sap 2000 results math well with the characteristics obtained from Structural Analysis Computer System (SACS) software.

6. DETERMINATION OF OPTIMAL PSDMS

All interested analyses are finally combined into PSDMs, through which the ground motion-specific IMs are related to the class-specific structural EDPs. Given the wide array of IMs and EDPs for every analysis, it was critical to select an optimal PSDM so as to narrow the amount of data processed. A selection of optimal IM–EDP pairs was made based on the criteria of practicality, effectiveness, efficiency and sufficiency.

Practicality: An IM-EDP pair is “practical” if it has some direct correlation to known engineering quantities and makes engineering sense.24 Specifically, IMs derived from known ground motion parameters and EDPs from resulting nonlinear analysis are practical. Correlation between analytical models and experimental data lend further practicality to the EDPs of the demand model. A further criterion for evaluating practicality is whether or not the IM is readily described by available attenuation relationships or other sources of hazard data.

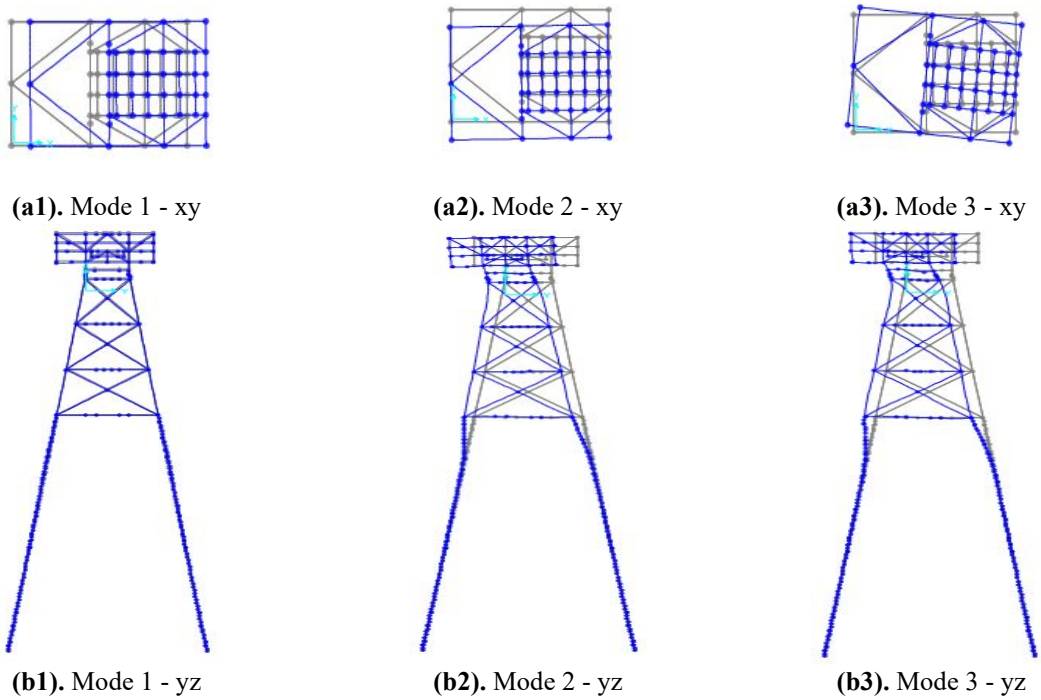

(a1). Mode 1 - xy **(a2).** Mode 2 - xy **(a3).** Mode 3 - xy

(b1). Mode 1 - yz **(b2).** Mode 2 - yz **(b3).** Mode 3 - yz

Figure 5. First three mode illustration of 3D modeled studied platform in (a). xy view and (b). yz view

Effectiveness: Effectiveness of a demand model is determined by the ability to evaluate Equation 1 in a closed form. For this to be accomplished, it was assumed the EDPs followed a log-normal distribution.20 Therefore an equation describing the demand model can be written as Equation 2.

$$EDP = a(IM)^b \quad (2)$$

To which a linear, or piecewise-linear, regression in log-log space can be applied to determine the coefficients (Eq. 3).

$$Ln(EDP) = A + B\,Ln(IM) \quad (3)$$

Efficiency: is the amount of variability of an EDP given an IM. Specifically, linear regression provides constants in Equation 3, as well as the distribution of data about the linear, or piecewise linear, fit. The measure used to evaluate the efficiency is the dispersion (Equation 4), defined as the standard deviation of the logarithm of the demand model residuals.[20] Equation 4 is for the case of a bilinear least squares fit. An efficient demand model requires a smaller number of nonlinear time-history analyses to achieve a desired level of confidence. Although it is not the only source of uncertainty, dispersion is a measure of randomness, or aleatory uncertainty.[56]

$$\sigma = \sqrt{\frac{\sum_{i=1}^{n}\left(ln\left(EDP_{i,fit}\right) - \ln\left(EDP_i\right)\right)^2}{n-3}} \quad (4)$$

Sufficiency: The PEER performance-based design framework achieves de-aggregation of the hazard and demand model if and only if the IM-EDP pair does not have a statistical dependence on ground motion characteristics, such as magnitude and distance. Such demand models with no conditional dependence are termed "sufficient".[51] A regression was performed on the IM–EDP pair residuals, conditioned on Mw and R to assess the sufficiency. A more rigorous definition of sufficiency can be used where the regression lines are ambiguous. The fitting of residual data is equivalent to the multivariate linear regression as can be seen in Eq. 5.

$$Ln(EDP) = A + BLn(IM) + C(M) + D(R) \quad (5)$$

Regarding the choice of IMs in the PSDMs, a number of important points should be considered. First, effectiveness and as a result of that, efficiency are not the only parameters for evaluating optimality, practicality and sufficiency should also be considered. Second, among the deemed optimal models which are practical, effective and sufficient, dispersion is the measure for considering which PSDM is the best. PSDMs with dispersions of 0.20–0.30 are superior, while the range 0.30–0.40 is still considered as reasonably acceptable.[18,52]

6.1 Engineering Demand Parameter Correlation

Recall the power-law formulation between EDPs and IMs. Based on this model, it is reasonable to speculate that different EDPs also can be related through a power-law model.[53] If such correlations exist, the number of EDPs can be reduced because two highly

correlated EDPs should provide very similar results in terms of optimal IM-EDP pairs. The coefficient of determination (R^2) is used to quantify the correlations between the studied EDPs in the logarithm space. Figure 6 indicates six sample charts in which EDP selection is randomized. These sample results of correlations have been chosen from the vast set of the platform model EDPs. Other models results are not presented for conciseness, however they generally show similar correlations among the EDPs. It is worth considering that, if presenting optimal IM-EDP pairs is done on a hit-or-miss basis, the arrangement is not going to achieve its desired objectives. As illustrated in Figure 6, it can be observed that, DR_{peak}–DR_{global} pair has relatively high correlation (R^2 = 0.8513), while some other EDP–EDP pairs indicate low correlation such as p_{soil} versus y_{soil} (R^2 = 0.0926).

Based on the results drawn from EDP correlation assessment and due to wide number of EDPs which can be contributed to develop PSDMs, 12 EDPs have been chosen. (However, all EDPs with low correlations have been employed to formulate the PSDMs)

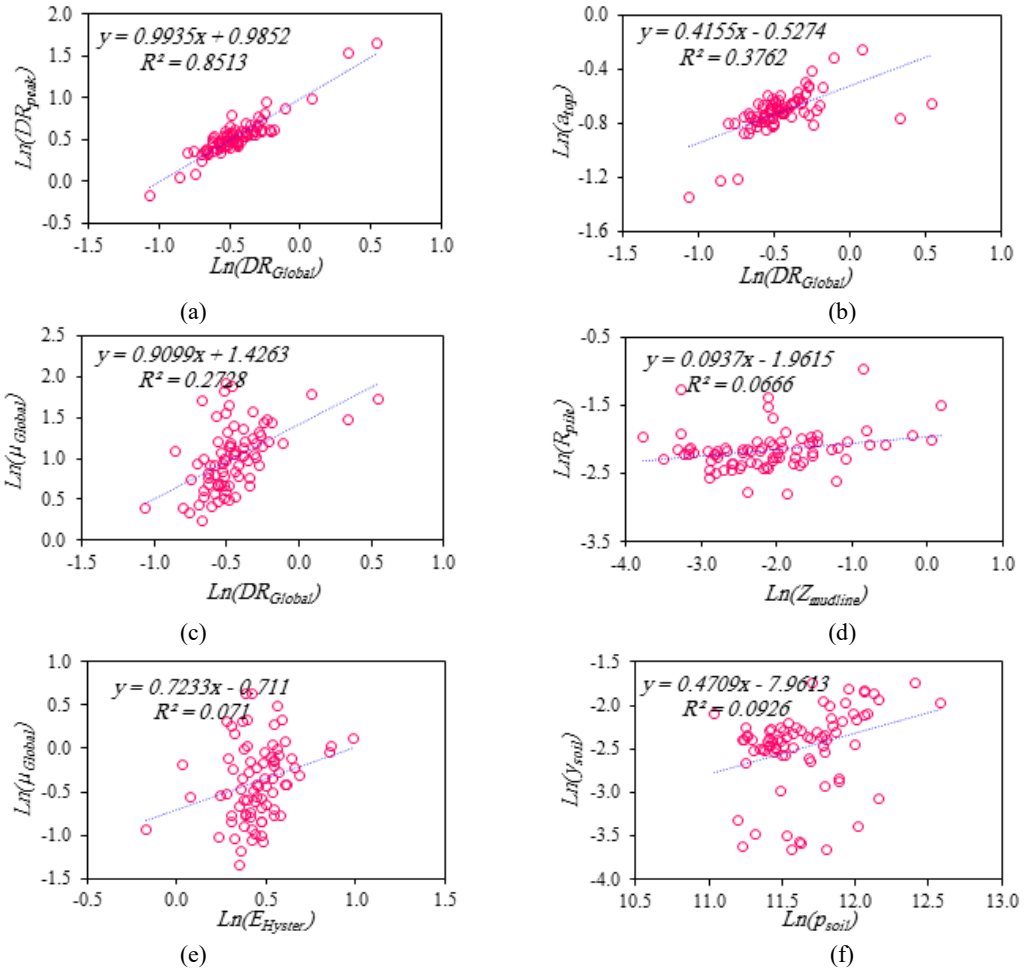

Figure 6. EDP correlation samples

6.2 Effectiveness and Efficiency Consideration of optimal PSDMs

The data were plotted in a log–log scale for each subsequent PSDM figure with EDP measures on the horizontal and IM measures on the vertical axes. This is a standard method for plotting any IM–EDP relationships. Based on the dependency of efficient property to effectiveness, the consideration of these properties of optimal PSDMs should be coupled simultaneously. The evaluation of effectiveness of IM–EDP pairs is possible using Equation 2 and plotting the PSDM in a log–log space. Certainly, the efficiency of PSDMs can be also seen for each IM–EDP pair diagrams of all models in the same trend. Dispersion of IM–EDP pairs is estimated by Equation 4 and by calculating the $EDP_{i,fit}$ based on the linear or piecewise-linear regression fit in a log–log space. Therefore, the efficiency assessment of PSDMs is possible. Figures 7-9 indicate (a) the effectiveness and (b) the efficiency of local, intermediate and global EDPs (based on Table 8) of the studied model, respectively. As illustrated in Figure 7, four local EDPs have been chosen and their effectiveness and efficiency vs. sixteen IMs, presented in Table 2, have been assessed. The considered EDPs are the top deck differential settlement, $Z_{top\ deck}$, and deck equipment acceleration, $a_{eq.}$, related to the deck part, the drift ratio on the working point elevation, $DR_{working\ point}$, of jacket part and the lateral displacement of soil in the vicinity of pile fixity point, y_{soil} which has been chosen from pile part. According to the charts it

can be comprehended that some IM-EDP pairs do not lead to effective results due to their low R^2 values. On the other hand, the indicated results of chart b states good efficiency of all of IM-EDP pairs in the range of selected local EDPs, based on the low value of σ.

Similarly, the effectiveness and efficiency of intermediate EDPs against IMs in the log-log space according to the power law is calculated and the result of four EDPs vs. IMs are plotted in Figure 8, a and b, respectively. The mudline elevation differential settlement, $Z_{z,mudline}$, and overall jacket drift ratio, DR_{Jacket}, are the intermediate EDPs which represent the response of whole jacket part. As so, below deck column axial force, F_{axial}, is the deck part demonstrative EDPs. Pile residual displacement, R_{pile}, has been selected in order to reflect the pile part seismic-induced behavior.

Indicated in Figure 8, a and b, it can be concluded that among selected intermediate EDPs, R_{pile} does not state effectiveness nor efficiency according to the low R^2 values and high dispersion which leads to σ values far from the upper efficiency limit (e.g. 0.4). Apart from that, for other intermediate PSDMs assessed here, it can be seen that although IM-EDP pairs are efficient, acceleration based IMs such as *PGA*, A_{rms}, I_a and *CAV* lead to non-effective PSDMs clearly. Moreover, displacement-related IMs (i.e. *PGD*) do not result in effective IM-EDP pairs.

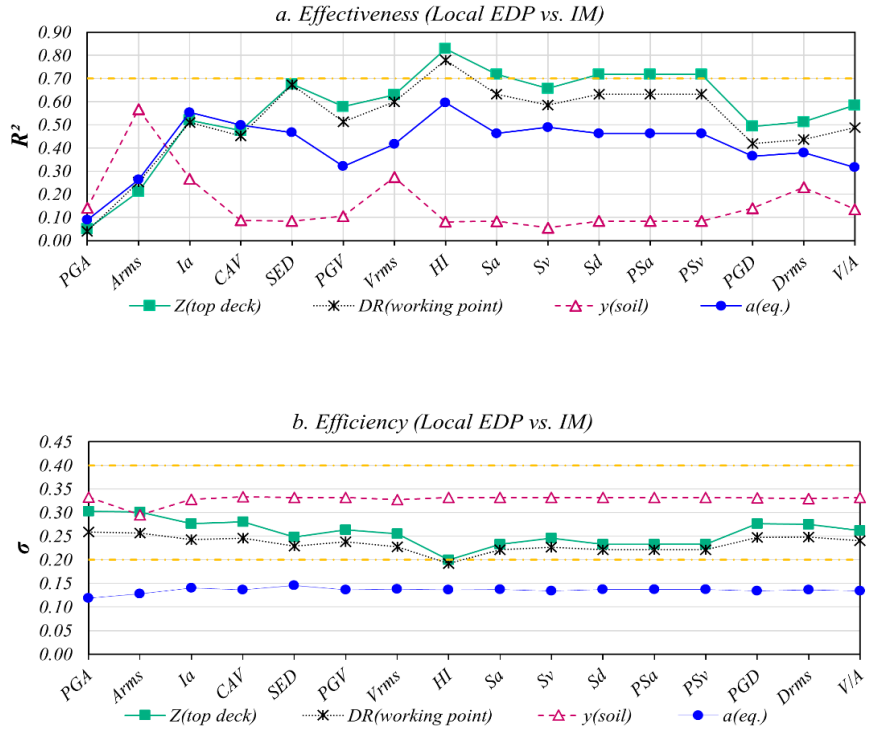

Figure 7. PSDM Assessment, Local EDPs vs. IMs (a) Effectiveness & (b) Efficiency

Among other IMs, the effectiveness of velocity related IMs against EDPs is considerable. The same conclusion has been drawn in both local and global EDP-IM pairs.

Figure 9, a and b, indicate the effectiveness and efficiency of IM-EDP pairs for global EDPs. As explained before, global EDPs are reflecting the behavior of whole structure or the effect of one main part to others which may lead to global structural response. As a sample, global drift ratio, DR_{Global}, global residual displacement index, RDI_{Global}, global ductility, μ_{Global}, and acceleration on top of the platform, a_{top}, have been evaluated. Plotted in Figure 9, the results of RDI_{Global} does not indicate high effectiveness nor the efficiency (except for V_{rms}-RDI_{Global}). As expressed before, in case of global EDPs, the acceleration-related IMs result in poor PSDMs due to low value of R^2.

Since this trend has been repeated in all three local, intermediate and global EDPs, for more specific evaluations the results of some of the IMs are not reflected hereafter based on poor established deductions and high dispersion which has been presented as low effectiveness and low efficiency. Moreover, since the effectiveness and efficiency results for $S_a(T_1, 5\%)$ and $S_d(T_1, 5\%)$ are the same as Pseudo Acceleration($PS_a(T_1, 5\%)$) and Pseudo Velocity ($PS_v(T_1, 5\%)$) respectively, only $S_a(T_1, 5\%)$ and $S_d(T_1, 5\%)$ results are reported instead henceforth for the purpose of brevity.

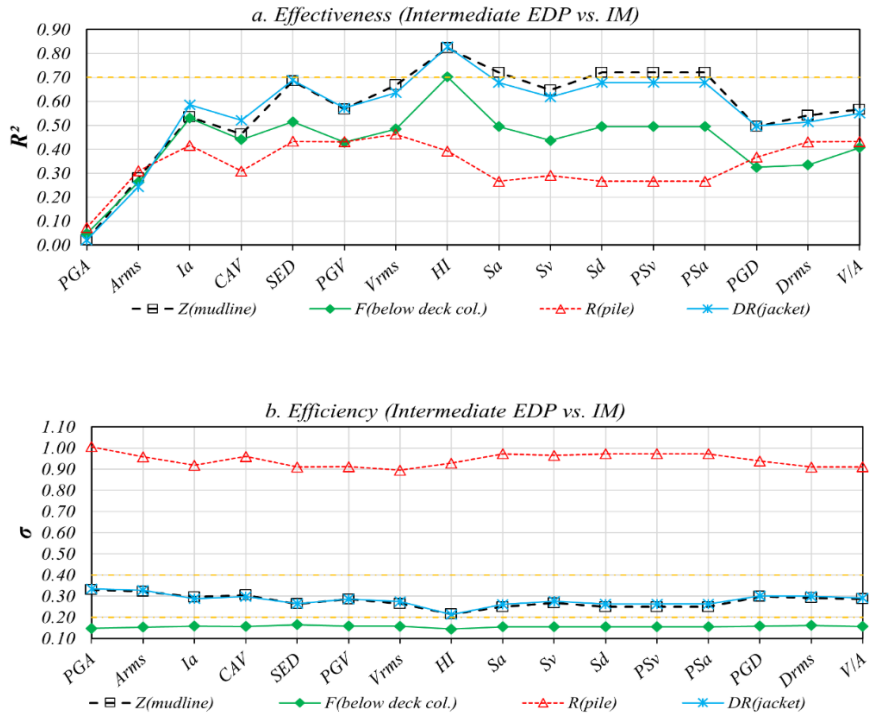

Figure 9. PSDM Assessment, Intermediate EDPs vs. IMs (a) Effectiveness & (b) Efficiency

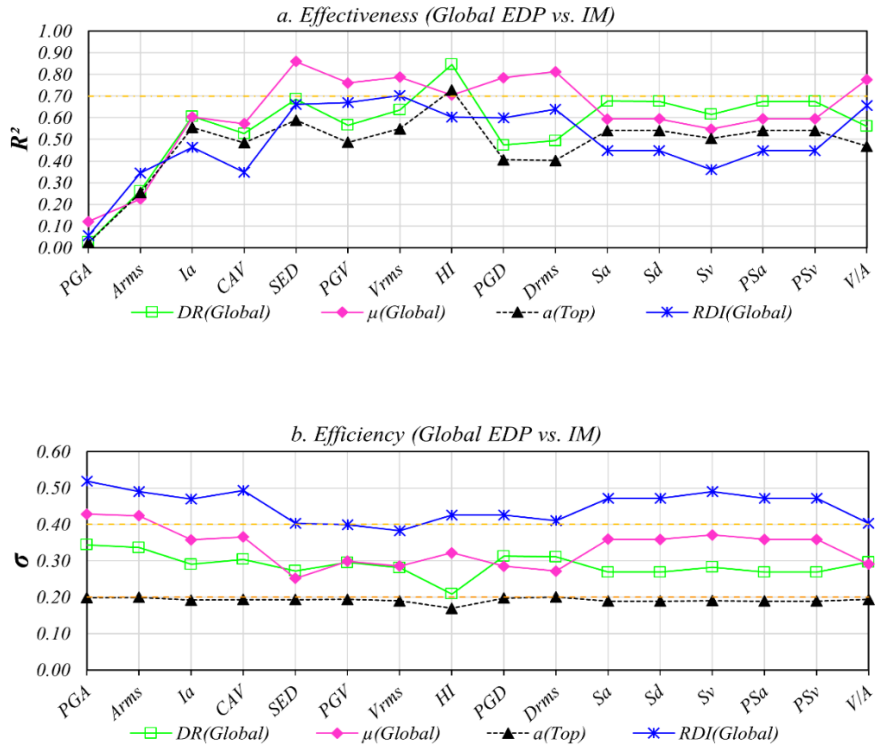

Figure 9. PSDM Assessment, Global EDPs vs. IMs (a) Effectiveness & (b) Efficiency

It can be seen that for the PSDMs provided by IM-DR_{Global}, *SED* and *HI*, lead to optimal IM-EDP pairs. However, V_{rms}, *PGV*, *V/A*, *PGD* and D_{rms} which do not represent optimal pairs in case of DR_{Global}, have indicated high effectiveness for μ_{Global}. These IMs are evaluated for selected EDPs more specifically in order to choose the optimal IM-EDP pairs which best reflect the effectiveness, efficiency, sufficiency and practicality. For this purpose, individual charts are

prepared each illustrates the IM vs. EDP in the log-log space.

Figure 10, indicates PSDMs in log-log space in which IM-EDP correlation, R^2, is calculated to represent the effectiveness of the chosen IM-EDPs. In Figure 10-a, *SED*-μ_{Global}, is an effective pair, while *SED*-R_{pile}, illustrated in Figure 10-b is a poor PSDM, based on R^2=0.4373. Thus, necessarily, an IM does not result in effective PSDMs for all EDPs.On the other hand, apart from employing $S_a(T_1, 5\%)$ in all recent researches for fragility analysis of fixed pile-founded offshore platforms, as shown in Figure 10-c, $S_a(T_1, 5\%)$-μ_{Global} effectiveness is evaluated and R^2=0.5698 is the indicator of poor effectiveness, while R^2=0.7657, which has been captured in Figure 10-d, is another evidence for effectiveness of another velocity-related IMs, *PGV*, vs. μ_{Global} of fixed pile-founded offshore platform.

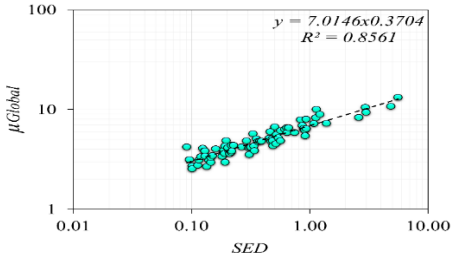

(a). *SED*-μ_{Global}

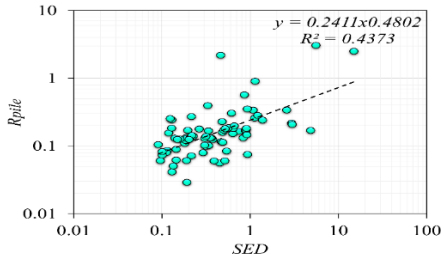

(b). *SED*-R_{pile}

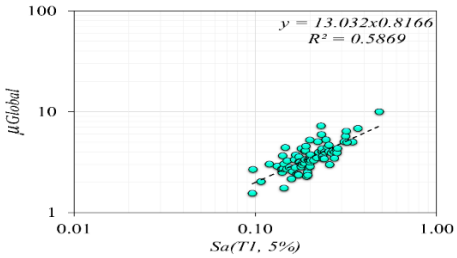

(c). $S_a(T_1, 5\%)$-μ_{Global}

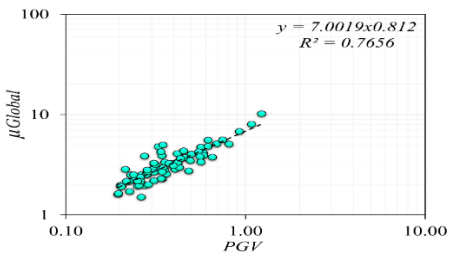

(d). *PGV*-μ_{Global}

Figure. 10. Effectiveness of Sample IM-EDP Pairs in log-log Space

Based on the results indicated in Figures 7 to 9, and Figure 10, it can be concluded that for each type of EDPs different IMs lead to generate optimal PSDMs. In other words, although *HI*-DR_{Global} represent the optimal IM-EDP pair, but *HI*-μ_{Global} does not reflect the most optimal PSDM comparing to *SED*-μ_{Global}.

On the other hand, the IMs which provide optimal PSDMs, mainly belong to the category of velocity-related IMs (except for μ_{Global} in which D_{rms} represent high effectiveness, too). It should be mentioned that among velocity-related IMs, $S_v(T_1, 5\%)$ does not reflect any optimal PSDMs in combination with EDPs, nevertheless.

It is worth noticing that, the superiority of velocity-related IMs is justifiable. While *PGA* exerts the greatest influence on the seismic response of structures with higher frequencies (periods of less than 0.5 s), structures with lower frequencies, (i.e. with periods of more than 0.5 s, are more sensitive to *PGV* and *PGD*). Besides, high-rise buildings studies indicated that due to high-rise response frequency range which is much wider than low-rise or mid-rise buildings, IMs such as spectral values $S_a(T1)$, $S_v(T1)$, $S_d(T1)$ and $PS_V(T1)$ represent only specific points in frequency content of the response spectrum.[18,54,55] For that reason, intensity measures comprising a wider range of frequency content of response spectra (e.g. *HI*) are more appropriate for the case of structures with periods more than 0.5 second. In this regard, based on the extensive evaluation carried out in this study on platform models, matrices of effectiveness, efficiency and sufficiency are utilized so as to reveal the optimal PSDMs from 16 studied IMs for various type of demand parameters.

Consequently, the results state that velocity-related IMs comprising wider range of frequency content for most of wide range of EDPs lead to optimal PSDMs. While $S_a(T_1, 5\%)$ is not among those IMs which result in optimal PSDMs for most various type of EDPs, it has been broadly used in current seismic fragility analysis of fixed pile-founded offshore platforms.

6.3 Sufficiency Consideration of optimal PSDMs

If the demand models do not have a statistical dependence on ground motion characteristics, such as M_w and R, they are considered "sufficient".[56] In order to evaluate the sufficiency, a regression analysis was performed on the IM–EDP pair residuals, conditioned on M_w and R. Figure 11-a,b and c, shows the regression plots for the residuals of three different PSDMs, generated in previous parts, based on Eq. 5 to assess the

sufficiency of the model. In each plot, trend line slope indicates the sufficiency of IM-EDP pair with respect to M_w (1) and R (2). As the trend line tends to be horizontal, the slope is lower and it reflects almost no statistical dependency on ground motion characteristics. For purposes of this paper, no residual dependency on 80% confidence interval is termed sufficient. The following plots have been chosen among all PSDM models and represented here while other PSDM plots are relinquished for brevity.

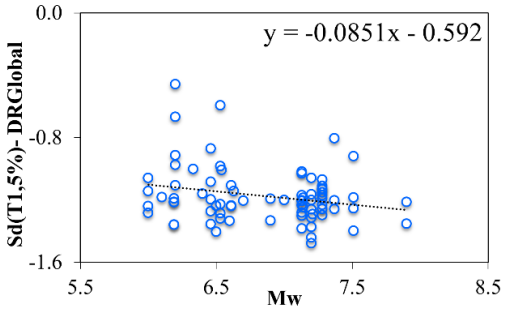

(a1). Sufficiency with Respect to M_w, C=0.0851

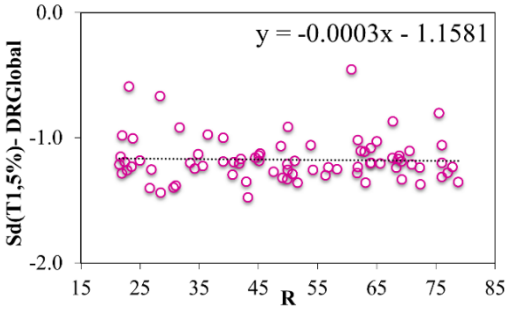

(a2). Sufficiency with Respect to R, D=0.0003

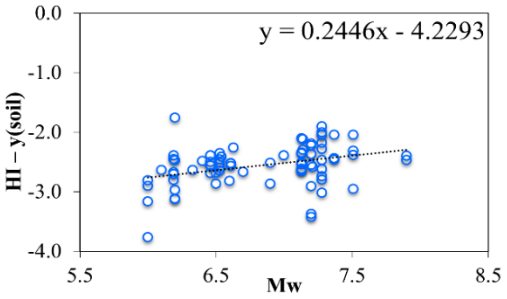

(b1). Sufficiency with Respect to M_w, C=0.2446

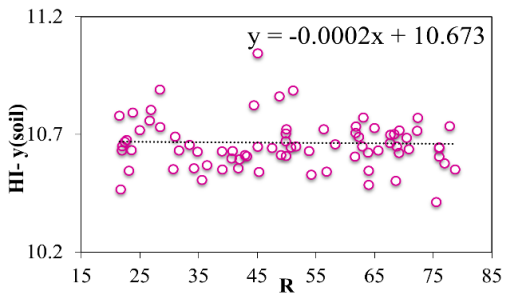

(b2). Sufficiency with Respect to R, D=0.0002

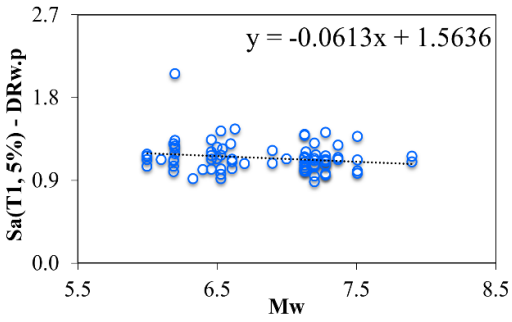

(c1). Sufficiency with Respect to M_w, C=0.0613

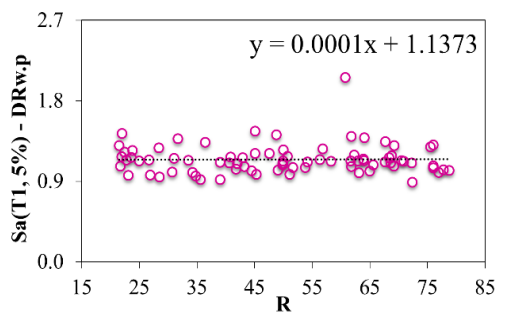

(c2). Sufficiency with Respect to R, D=0.0001

Figure 11. PSDM Sufficiency Assessment Sample Plots

Figure 11-a indicates the results of sufficiency of $S_d(T_1,5\%)$-DR_{Global} as an IM-EDP pair. The selected IM is a displacement-related IM and the EDP is chosen from the group of global engineering demand parameter. As it can be seen, the IM-EDP pair selected in this figure considered sufficient since the C value is 0.0851 and D is 0.0003. However, the practicality assessment is the final issue to be taken into consideration.

Among intermediate engineering demand parameters, max soil displacement is selected and sufficiency of this EDP versus *HI* is evaluated. The results are plotted in Figure 11-b and the coefficients of C and D are calculated. The *HI*-y_{soil} is considered poor due to its C value equals to 0.2426 which does not reflect low dependency to ground motion magnitude, while it is deemed sufficient with respect to R owing to D = 0.0002. Nevertheless, according to the results illustrated in Figure 8, the selected PSDM is neither effective nor efficient.

In accordance with other sufficiency assessment plots, Figure 11-c, illustrate C and D values achieved by considering the drift of jacket top story (working point elevation), $DR_{working\ point}$, as a local EDP, and $S_a(T_1,5\%)$, as an structure-specific, acceleration-related IM. C and D values are 0.0613 and 0.0001, respectively. According to low slopes, $S_a(T_1,5\%)$- $DR_{working\ point}$ is

deemed sufficient, while it has not satisfied the effectiveness as shown in Figure 7.

Table 10, also listed R^2, σ, C and D values of 10 IMs against two sample global EDPs so as to reveal the effectiveness, efficiency and sufficiency of these PSDMs based on Eq. 2, 4 and 5. Expressing R^2, σ, C and D values in a table, provide a quantitative tool and facilitate the comparison.

6.4 Practicality Consideration of Optimal PSDMs

Aforementioned in previous parts, an IM-EDP pair is "practical" if it has some direct correlation to known engineering quantities and makes engineering sense. For instance, though the traditional relation between *PGA* and structural response is practical, but *PGA* is neither efficient nor effective across larger period ranges (e.g. in case of high-rises and offshore platforms). The classification of practicality is, unfortunately, a subjective exercise. According to the recent researches, a clearly practical EDP is drift ratio. Besides, other EDPs assessed in this paper have been chosen among known engineering quantities. It is worth noticing that since probabilistic seismic demand model for fixed pile-founded offshore platforms has not performed yet, representing other IM-EDP pairs apart from those employed for building and bridges is not abnormal.

Table 10: R^2, σ, C and D values of 10 IMs against two sample global EDPs

IM Type		IM	R^2*	σ**	C***	D***
EDP : DR_{Global}						
Non-Structure Specific	Acceleration-Related	***CAV***	0.53	0.30	0.1225	0.0007
		SED	0.69	0.27	0.1232	0.0017
	Velocity-Related	***PGV***	0.57	0.30	0.1304	0.0012
		Vrms	0.64	0.28	0.1213	0.0021
	Displacement-Related	D_{rms}	0.49	0.31	0.1695	0.0012
	Time-Related	V_{max}/A_{max}	0.56	0.30	0.1330	0.0012
Structure-Specific	Acceleration-Related	$S_a(T_1,5\%)$	0.68	0.27	0.0865	0.0005
	Velocity-Related	$S_v(T_1,5\%)$	0.62	0.28	0.1017	0.0004
		HI	0.85	0.21	0.0736	0.0002
	Displacement-Related	$S_d(T_1,5\%)$	0.68	0.27	0.0851	0.0003
EDP : μ_{Global}						
Non-Structure Specific	Acceleration-Related	***CAV***	0.57	0.37	0.1550	-0.0027
		SED	0.86	0.25	0.1445	0.0008
	Velocity-Related	***PGV***	0.76	0.30	0.1255	0.0002
		Vrms	0.79	0.29	0.1475	0.0014
	Displacement-Related	***PGD***	0.79	0.29	0.0303	0.0005
		D_{rms}	0.81	0.27	0.0231	0.0006
	Time-Related	V_{max}/A_{max}	0.78	0.29	0.1180	0.0003
Structure-Specific	Acceleration-Related IMs	$S_a(T_1,5\%)$	0.59	0.36	0.2078	-0.0012
	Velocity-Related IMs	$S_v(T_1,5\%)$	0.55	0.37	0.1907	-0.0013
		HI	0.71	0.32	0.2221	-0.0009
	Displacement-Related IMs	$S_d(T_1,5\%)$	0.59	0.36	0.2079	-0.0012

* Effectiveness ** Efficiency

*** **C**: Sufficiency with Respect to M_w, **D**: Sufficiency with Respect to R

7. Optimal IM-EDP Pairs

Summing up the study, the optimal IM-EDP pairs for typical South Pars platforms located in the Persian Gulf are listed in the Table 10, in which the effectiveness, efficiency and sufficiency are included. Global, intermediate and local EDPs are separated and the results are presented individually.

It can be seen that for each EDP type (ductility, drift, acceleration, etc.) the IMs which lead to optimal PSDMs are not necessarily the same. While *SED*

provide optimal PSDM for global ductility, *HI* is the first IM among those which provide optimal PSDMs for other EDP types. However, it is clearly concluded that, velocity-related IMs result in optimal PSDMs.

Table 11. Ranking of Optimal IM-EDP Pairs

	Global PSDMs	Intermediate PSDMs	Local PSDMs
1	SED-μ_{Global}	HI-DR_{jacket}	HI-$Z_{topdeck}$
2	HI-DR_{Global}	HI-$Z_{mudline}$	HI-$DR_{working\ point}$
3	D_{rms}-μ_{Global}	$S_d(T_1,5\%)$-$Z_{mudline}$ $S_a(T_1,5\%)$-$Z_{mudline}$	$S_d(T_1,5\%)$-$Z_{topdeck}$ $S_d(T_1,5\%)$-$Z_{topdeck}$
4	V_{max}/A_{max}-μ_{Global}	HI-F_{axial}	
5	V_{rms}-μ_{Global}		
6	PGV-μ_{Global}		
7	HI-a_{top}		

8. Conclusion

Optimal IM-EDP pairs for typical fixed pile-founded offshore platforms located in the South Pars, Persian Gulf, have been thoroughly investigated employing PSDA. For nonlinear time history analysis of the platform 3D model, 80 ground motion records, based on bin approach, have been selected. PSDMs for all 16 IMs vs. wide range of EDPs in levels of local, intermediate and global are build. Based on practicality, effectiveness, efficiency and sufficiency, the optimal PSDMs are extensively assessed and optimal IM–EDP pairs are denoted. The following conclusion are drawn:

- Based on the type of EDPs (e.g. ductility, drift, acceleration, etc.) the IMs which lead to optimal PSDM vary.
- Generally, velocity-related IMs are more appropriate than acceleration, displacement and time-related ones.
- Based on the comprehensive evaluation on the metrics of effectiveness, efficiency, practicality and sufficiency: *HI*, for drift, top acceleration, differential settlement and deck column axial forces demand parameters, and *SED* for ductility, result in optimal PSDMs for the probabilistic seismic demand analysis of the studied structures.
- In contrast, the widely used $S_a(T_1,5\%)$, for probabilistic assessment and fragility estimation of fixed pile-founded offshore platforms, is not an appropriate IM, due to its unconvinced performance with regard to low effectiveness.

As a final conclusion, HI-DR_{Global} and SED-μ_{Global} for global EDP level, HI-DR_{Jacket} for intermediate level and HI-$Z_{topdeck}$ for local level is proposed as the optimal PSDMs for typical South Pars fixed pile-founded offshore platforms and recommend to be used for future studies.

9. References

1- Yasseri, S.F., Ossei, R., (2004), *Seismic fragility analysis of pile-founded offshore platforms*, Proc. International Offshore and Polar Eng. Conference, Toulon, France.

2- El-Din, M. N. and Kim, J., (2014), *Seismic performance evaluation and retrofit of fixed jacket offshore platform structures*, J. Performance of Constructed Facilities.

3- Cornell, CA., (1995), *Structural reliability-some contributions to offshore technology*, Proceedings of the Offshore Technology Conference, 7753. Paper OTC.

4- ISO. (2004), ISO 19902 petroleum and natural gas industries-fixed steel offshore structures. International Organization for Standardization.

5- Ronalds, B.F., Trench, D.J., Pinna R., (2007), *On the relationship between platform topology, topside weight and structural reliability under storm overload*. J. Constr. Steel Res., 63(8):1016–23.

6- Asgarian, B., Aghakouchak, A. A., Alanjari, P. and Assareh, M. A., (2008), *Incremental Dynamic Analysis of Jacket Type Offshore Platforms Considering Soil-Pile Interaction*, 14th World Conference on Earthquake Engineering, Beijing China.

7- Vamvatsikos, D., (2002), *Seismic Performance Capacity and Reliability of Structures as Seen through Incremental Dynamic Analysis*, Ph.D. Thesis. Department of Civil and Environmental Engineering, Stanford University, Stanford, CA.

8- Ajamy A., Zolfaghari M.R., Asgarian B., Ventura C.E., (2014), *Probabilistic seismic analysis of offshore platforms incorporating uncertainty in soil–pile–structure interactions*, J. Constr. Steel Res.; 101, 265–279.

9- Elsayed, T., El-Shaib, M., Gbr, k., (2014), *Reliability of fixed offshore jacket platform against earthquake collapse*, J. Ships Offshore Struct., Vol.11 (2), p. 167–181.

10- Anderson, T.W., & Darling, D.A., (1954), *A test of goodness-of-fit*, J. Am. Stat. Assoc, Vol. 49, p.765–769.

11- Abyani, M., Asgarian, B., Zarrin, M., (2017), *Statistical assessment of seismic fragility curves for steel jacket platforms considering global dynamic instability,* J. of Ships and Offshore Struc., Vol.13 (4), p. 366–374.

12- Abyani, M., Bahaari, M. R., Zarrin, M., & Nasseri, M. (2019), *Effects of sample size of ground motions on seismic fragility analysis of offshore jacket platforms using Genetic Algorithm*, J. Ocean Eng., Vol. 189.

13- Cornell, CA., & Krawinkler, H., (2000), *Progress and challenges in seismic performance assessment*, PEER Center News, Vol.3(2).

14- Shome, N., (1999), *Probabilistic Seismic Demand Analysis of Nonlinear Structures*. PhD. Thesis, Dep. Civil and Envir. Eng. Stanford University, Stanford, CA.

15- Shome, N., and Cornell, C.A., (1999), *Probabilistic seismic demand analysis of nonlinear structures*, Reliability of Marine Structures Report No. RMS-35, Dept. of Civil and Envir. Engineering, Stanford University, California.

16- Luco, N., (2002). *Probabilistic seismic demand analysis, SMRF connection fractures, and near-source effects*. Ph.D. Thesis. Dep. Civil and Environ. Eng. Stanford University, Stanford, CA.

17- Gardoni, P., Der Kiureghian, A., & Mosalam, K.M., (2002), *Probabilistic capacity models and fragility estimates for reinforced concrete columns based on experimental observations*, J. Eng. Mech., Vol. 128(10), p. 1024–1038.

18- Mackie, K., & Stojadinovic, B., (2003), *Seismic demands for performance-based design of bridges*, PEER 2003/16 Report, PEER Center, California.

19- Gardoni, P., Mosalam, K.M., & Der Kiureghian, A., (2003), *Probabilistic seismic demand models and fragility estimates for RC bridges*, J. Earthq. Eng., Vol. 7(1), p. 79–106.

20- Zhong, J., Gardoni, P., Rosowsky, D., & Haukaas, T., (2008), *Probabilistic seismic demand models and fragility estimates for reinforced concrete bridges with two-column bents*, J. Eng. Mech., Vol. 134(6), p. 495–504.

21- Huang, Q., Gardoni, P., & Hurlebaus, S., (2010), *Probabilistic seismic demand models and fragility estimates for reinforced concrete highway bridges with one single-column bent*, J. Eng. Mech., Vol.136(11), p. 1340–1353.

22- Padgett, J. E., Neilson, B. G., & DesRoches, R., (2008), *Selection of Optimal Intensity Measures in Probabilistic Seismic Demand Models of Highway Bridge Portfolios*, J. Earthq. Eng. Struc. Dyn., Vol.37.

23- Werner, S.D., Rix, G.J., & DesRoches, R., (2008), *Seismic risk management for seaports*, Paper presented at the 14th World Conference on Earthquake Engineering, Beijing, China.

24- Rix, G.J., Burden, L., & Werner, S.D., (2009), *Seismic risk management for port systems*, TCLEE Conference, Oakland, CA.

25- Werner, S.D., DesRoches, R., Rix, G.J., & Shafieezadeh, A., (2009), *Fragility models for container cargo wharves*, Paper presented at the TCLEE 2009 Conference, Oakland, CA.

26- Yang, C.W., DesRoches, R., & Rix, G.J., (2012), *Numerical fragility analysis of vertical-pile-supported wharves in the western United States*, J. Earthq. Eng.m Vol.16(4), p. 579–594.

27- Shafieezadeh, A., (2011), *Seismic vulnerability assessment of wharf structures*, Ph.D. dissertation. Georgia Institute of Technology, Atlanta, GA.

28- Amirabadi, R., Bargi, Kh., Dolatshahi, M., Heidary Torkamani, H., & Maccullough, N., (2014), *Determination of optimal probabilistic seismic demand models for pile-supported wharves*, Structure and Infrastructure Engineering: Maintenance, Management, Life-Cycle Design and Performance, Vol. 10(9), p. 1119-1145.

29- Berahman, F. and Behnamfar, F., (2009), *Probabilistic Seismic Demand Model and Fragility Estimates for critical Failure modes of Un-Anchored Steel Storage Tanks in Petroleum Complexes*, J. Probabilistic Eng. Mech. Elsevier, Vol. 24, p.527-536.

30- Lucchini, A., Franchin, P., & Mollaioli, F., (2015), *Probabilistic Seismic Demand. Model for Nonstructural Components*, Earthq. Eng. Struc. Dyn., Vol. 45, p. 599-617.

31- Hariri-Ardebili, M. A. and Saouma, V. E., (2016), *Probabilistic Seismic Demand Model and Optimal Intensity Measure for Concrete Dams*, J. Struct. Safety, Elsevier, Vol. 59, p. 67-85.

32- Kaynia, A. M., (2019), *Seismic Consideration in Design of offshore Wind Turbines*, Journal of Soil Dynamics and Earthquake Engineering, 124, 399-407.

33- Kia M., Amini A., Bayat M. and Ziehl P., (2020), *Probabilistic Seismic Demand Analysis of Structures Using Reliability Approaches*, Journal of Earthquake and Tsunami, https://doi.org/10.1142/S1793431121500111

34- American Petroleum Institute, (2000), Recommended practice for planning, designing and constructing fixed offshore platforms. API Recommended Practice 2A (RP-2A). 21st ed. American Petroleum Institute, Washington, D.C.

35- Shome, N., Cornell, C.A., Bazzurro, P., & Caraballo, J.E., (1998), *Earthquakes, records, and nonlinear responses*. Earthquake Spectra, 14(3), 467–500.

36- Foutch, D.A., Yu, C.Y., & Wen, Y.K., (1992), Reliability of steel frame buildings under seismic load. 10th World Conference on Earthq. Eng., Rotterdam, Netherlands.

37- Pacific earthquake engineering research center., (2006), PEER NGA Database. Berkeley: University of California, [http://peer.berkeley.edu/nga/].

38- NEHRP., (2001), NEHRP recommended provisions for seismic regulations for new buildings and other structures, Washington, DC, USA: Building Seismic Safety Council.
39- Kramer, SL., (1996), Geotechnical earthquake engineering. Upper Saddle River, NJ.
40- Matlock, H., (1970), *Correlations for Design of Laterally Loaded Piles in Soft Clay*, Second Annual Offshore Technology Conference, Houston, Vol.1204, p. 557 - 594.
41- Reese, L. C., & Cox, W. R., (1975), *Field Testing and Analysis of Laterally Loaded Piles in Stiff Clay*, Offshore Technology Conference, OTC 2312.
42- O'Neill, M. W., & Murchinson, J. M., (1983*), An Evaluation of p-y Relationships in Sands*, A Report to the American Petroleum Institute.
43- Wesselink, B.D., Murff, J.D., Randolph, M.F., Nuenz, I.L & Hyden, A.M., (1988), *Analysis of Centrifuge Model Test Data from Laterally Loaded Piles in Calcareous Sand*, Conference Paper, p. 261-269, Engineering for Calcareous Sediments, Jewell & Andrews Eds.
44- Sap 2000, (2005), Structural Analysis Program, Analysis Reference Manual, Computers and structures, Inc., Berkeley, California, USA.
45- American Petroleum Institute, (2008), Recommended Practice for Planning, Designing and Constructing Fixed Offshore Platforms - Working Stress Design. API recommended practice (RP-2A-WSD), 21st Edition, Errata and Supplement.
46- Anagnostopoulos, H. G., (1983), *Cyclic Axial Pile Response—Alternative Analyses*. Proceedings of the Conference on Geotechnical Practice in Offshore Engineering, ASCE, Austin, Texas.
47- Coyle, H.M. and Suliaman, I.H., (1967), *Skin Friction for Steel Piles in Sand. Journal of the Soil Mechanics and Foundation Division*, Proc., American Society of Civil Engineers, Vol. 93(SM6), p. 261–278.
48- Reese, L. C. and O'Neill, M., (1971), *Criteria for Design of Axially Loaded Drilled Shafts*. Center for Highway Research Report, University of Texas.
49- Rathje EM, Kottke RA, Trent WL., (2010), *Influence of input motion and site property variabilities on seismic site response analysis*, J Geotech. Geoenviron. Eng. ASCE, Vol. 136(4).
50- Hashash, Y., Groholski, D., Phillips, C., Park, D., & Musgrove M., (2012), DEEPSOIL 5.1. User Manual and Tutorial.
51- Cornell, C.A., Jalayer, F., Hamburger, R.O., & Foutch, D.A., (2002), *Probabilistic basis for 2000 SAC/FEMA steel moment frame guidelines*. J. Struct. Eng. April, Vol. 128(4), 526–533.
52- Mollaioli, F., Lucchini, A., Cheng, Y., & Monti, G., (2013), *Intensity measures for the seismic response prediction of base-isolated buildings*. Bull Earthq. Eng., Vol. 11(5):1841–1866.
53- Wang, X., Shafieezadeh, A., & Ye, A., (2018) *Optimal intensity measures for probabilistic seismic demand modeling of extended pile-shaft-supported bridges in liquefied and laterally spreading ground*, Bull Earthquake Eng.
54- Ji, J., Elnashai, A.S., Kuchma, D.A., (2007), *Seismic fragility assessment for reinforced concrete high-rise buildings* - Report 07-14, Mid-America Earthquake Center, University of Illinois at Urbana-Champaign.
55- Pejović, J and Jancović, S., (2015), *Dependence of high-rise buildings response on the earthquake Intensity*. GRADEVINAR; Vol. 67(8), p. 749-759.
56. Reed JW, Kassawara RP., (1990), *A criterion for determining exceedance of the operating basis earthquake,* Nucl. Eng. Des.; Vol.123, p. 387–396.
57- Arias A., (1970), *A measure of earthquake intensity*. In: Hansen RJ (ed) Seismic Design for Nuclear Power Plants. MIT Press, Cambridge, p. 438–483.
58- Housner GW., (1959), *Behavior of structures during earthquakes*, J. Eng. Mech Div; Vol. 85, p. 109–130